Fusion of Non-Contacting Sensors and Vital Parameter Extraction Using Kalman Filtering

Jérôme Foussier, Daniel Teichmann, Jing Jia, Steffen Leonhardt

Abstract—**This paper describes the implementation of a Kalman Filter to separate heart rate and respiratory activity out of a signal that has been acquired by three different sensors in parallel. The different techniques of sensor fusion, signal extraction and signal shaping are merged into one single state space model. It can be demonstrated, assuming sine shaped signals for heart and breathing activity, that the processing performs well when the heart and breathing rate are approximately estimated. In addition, real-time processing ability has been evaluated and achieved.**

Index Terms—**non-contacting sensors, kalman filter, sensor fusion, vital parameter extraction.**

I. Introduction

KALMAN Filtering techniques can be used either for *sensor fusion*, *signal extraction* or *signal shaping*. All three methods have been included into one single set-up. In this case, a linearised state space model has been used for calculations. The applied methods are able to extract breathing and heart activities out of signals that have been acquired prior to that (c.f. chapter III).

R.E. Kalman et al. [1] firstly introduced this filtering technique based on the Wiener Filter [2]. The aim of these filters is to minimise the squared error between real and estimated signal with the constraint to minimise the variance as well. With the aid of a-priori knowledge and the modelling of noise processes, the Kalman Filter offers good properties for the efficient implementation on computers. In addition, the overall structure is straightforward. Q. Lee et al. [3] used Kalman Filters for robust heart rate estimation. Other examples for signal filtering processes can be found in [4], [5] and [6].

M. Mneimneh et al. [4] compared different approaches to remove ECG baseline wandering and found for the Kalman Filter that it returned best results comparing the mean error and its standard deviation.

O. Sayadi et al. [5] used a modified, more complex, Kalman Filter structure to de-noise and compress ECG data by estimating parameters of a combination of gaussian basis functions.

A. Schlögl et al. [6] de-trended heart rate variability (HRV) data to obtain the mean heart rate and do further analysis.

All these examples show that Kalman Filters can be widely employed in the field of (biomedical) signal processing. The good results and the easy implementation motivates the use of such a system.

Manuscript received March 22nd, 2011; revised April 4th, 2011.
J. Foussier, D. Teichman and S. Leonhardt are with the Philips chair for Medical Information Technology (MedIT), RWTH Aachen University, 52074 Aachen, Germany, emails: {foussier, teichmann, leonhardt}@hia.rwth-aachen.de (see http://www.medit.rwth-aachen.de)
J. Jia is with RWTH Aachen University, email: jing.jia@rwth-aachen.de
This work was partly funded by HeartCycle, an EU-project about compliance and effectiveness in HF and CHD closed-loop management.

II. Kalman Filtering

The three introduced methods in the Kalman Filtering process can be described by a simple block diagram shown in Fig. 1. Three different sensors S1 to S3 on the left hand side represent the inputs of the system. On the right hand side, five different signals are extracted, the breathing as well as heart activity and three offset signals that describe the absolute signal amplitude of the sensors, respectively. Recursive estimation algorithms, such as the Kalman Filter, are very accurate in the estimation of signal levels and show good performance when compared to non-recursive estimation algorithms. In addition, they are easy to implement. With each time step, more and more information about the system is gathered, since the variance is minimised. The strongest drawback is the need of accurate knowledge about the measurement system, noise and signal shapes [7]. In many cases, it is not trivial to obtain this knowledge for a real system and it has to be approximated, which compulsorily leads to a decrease in performance.

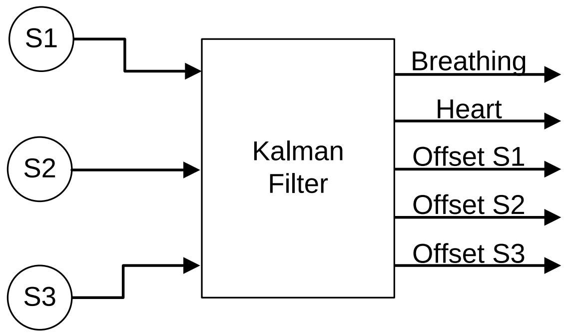

Fig. 1. Kalman Filter Sensor Fusion (Sensors: S1 to S3) and Vital Signs Extraction

A. General Equations

Usually, using the state vector $\mathbf{x_k} \in \Re^N$ and the measurement vector $\mathbf{z_k} \in \Re^M$ (see (2)), the equations for the Kalman filter are set up in a state space model, see (1). System and measurement noise are modelled by the vectors $\mathbf{w_k}$ and $\mathbf{v_k}$. They are assumed to be normally distributed, mean valued around zero (white noise) and statistically independent from each other. The covariance matrices of the noise vectors are called $\mathbf{Q}$ and $\mathbf{R}$, respectively. $\mathbf{u_k}$ is an optional input vector, which is related via $\mathbf{B}$ to the state vector $\mathbf{x_k}$. The state transition matrix $\mathbf{A}$ relates the previous state $\mathbf{x_{k-1}}$ to the actual state $\mathbf{x_k}$. Furthermore, the measurement matrix $\mathbf{H}$ connects the current state to the measurement vector. In general, the matrices $\mathbf{A}$, $\mathbf{B}$, $\mathbf{H}$, $\mathbf{Q}$ and $\mathbf{R}$ are time variant, so that they have to be recalculated at each time step. In a slowly or never changing system, some or all of them can be assumed as constant or only have to be updated after some time steps.

$$\mathbf{x_k} = \mathbf{A}\mathbf{x_{k-1}} + \mathbf{B}\mathbf{u_{k-1}} + \mathbf{w_{k-1}} \tag{1}$$

$$\mathbf{z_k} = \mathbf{H}\mathbf{x_k} + \mathbf{v_k} \tag{2}$$

The state vector $\mathbf{x_k}$ is unknown, but can be determined by using a-priori ($\hat{\mathbf{x}}_\mathbf{k}^-$) and a-posteriori ($\hat{\mathbf{x}}_\mathbf{k}$) estimations. The estimation errors are defined as $\mathbf{e}_\mathbf{k}^- = \mathbf{x_k} - \hat{\mathbf{x}}_\mathbf{k}^-$ and $\mathbf{e_k} = \mathbf{x_k} - \hat{\mathbf{x}}$. The corresponding covariance matrices are named $\mathbf{P}_\mathbf{k}^-$ and $\mathbf{P_k}$.

The estimated vector $\hat{\mathbf{x}}_\mathbf{k}$ is calculated by building the linear combination of the a-priori knowledge ($\hat{\mathbf{x}}_\mathbf{k}^-$) weighted difference between the actual measurement $\mathbf{z_k}$ and the predicted state $\mathbf{z_k} - \mathbf{H}\hat{\mathbf{x}}_\mathbf{k}^-$ in (3). With the system noise covariance matrix $\mathbf{Q}$ and the estimation error covariance matrix $\mathbf{P_{k-1}}$, taken from the previous time step, it is possible to calculate an a-priori estimation error matrix $\mathbf{P}_\mathbf{k}^-$, see (4). $\mathbf{K_k}$ is known as the Kalman Gain. Its calculations in (5) use the a-priori error covariance matrix $\mathbf{P}_\mathbf{k}^-$ and the noise covariance matrix $\mathbf{R}$ as well as the measurement matrix $\mathbf{H}$. Afterwards, the estimation error covariance matrix $\mathbf{P_k}$ is calculated (6).

$$\hat{\mathbf{x}}_\mathbf{k} = \hat{\mathbf{x}}_\mathbf{k}^- + \mathbf{K_k}(\mathbf{z_k} - \mathbf{H}\hat{\mathbf{x}}_\mathbf{k}^-) \tag{3}$$

$$\mathbf{P}_\mathbf{k}^- = \mathbf{A}\mathbf{P_{k-1}}\mathbf{A^T} + \mathbf{Q} \tag{4}$$

$$\mathbf{K_k} = \mathbf{P}_\mathbf{k}^-\mathbf{H^T}(\mathbf{H}\mathbf{P}_\mathbf{k}^-\mathbf{H^T} + \mathbf{R})^{-1} \tag{5}$$

$$\mathbf{P_k} = (\mathbf{I} - \mathbf{K_k}\mathbf{H})\mathbf{P}_\mathbf{k}^- \tag{6}$$

Even with time-invariant system matrices the Kalman Gain $\mathbf{K_k}$ is time-variant as it depends on the estimation error covariance matrix, which changes at each calculation step. Furthermore, two special cases can be considered:

- the predicted is more trustworthy than the actual state $\mathbf{Q} \to \mathbf{0} \Rightarrow \mathbf{K_k} \to \mathbf{0}$
- the measurement is more trustworthy than the actual state $\mathbf{R} \to \mathbf{0} \Rightarrow \mathbf{K_k} \to \mathbf{H^{-1}}$

In measurement systems, the calculations are divided into two steps, the *Measurement Update (mud)* and the *Time Update (tud)*, see Fig. 2. During *tud* the internal state vector $\hat{\mathbf{x}}_\mathbf{k}^-$ is estimated (prediction). Afterwards, during *mud*, the measurement vector $\mathbf{z_k}$ is taken into account and aligned with the prediction.

At this point, it is already noticeable that the Kalman Filtering is on the one hand able to be used as a sensor fusion system and on the other as a signal extraction system. This will be further elaborated in the following chapters II-B and II-C

B. Sensor Fusion

In general, fusion of different signals need an expansion of the measurement matrix $\mathbf{H}$ to the number of employed sensors and then has to be linked to the state vector $\mathbf{x_k}$. Systematic analysis of Kalman Filters applied in de-centralised and centralised fusion layers have already been modelled and analysed in [10]. Simulated data is biased with linear as well as non-linear functions and performance of the different fusion layers is evaluated. Also the effect of having a defective or broken sensor is analysed.

In this case the fusion occurs on a centralised layer as all input signals are routed to one single processing filter. No pre-filtering is applied.

In a first instance, the state transition matrix and its corresponding state vector have to be determined. The detailed derivation of the state transition matrix $\mathbf{A}$ and the state vector $\mathbf{x_k}$ can be found in the appendix in the case of one sensor and one signal that has to be extracted. Two vital signals, which can be approximated by sine shaped signals (breathing X_s/V_s and heart beat X_f/V_f) and three different sensors with different offsets ($C_{1,k}$-$C_{3,k}$), are included in this setup. Therefore the state vector and the state transition matrix taken from Eqs. (17) and (18) have to be expanded:

$$\mathbf{x_k} = \begin{pmatrix} X_{f,k} \\ V_{f,k} \\ X_{s,k} \\ V_{s,k} \\ C_{1,k} \\ C_{2,k} \\ C_{3,k} \end{pmatrix}, \tag{7}$$

$$\mathbf{A} = \begin{pmatrix} 1 & \Delta t & 0 & 0 & 0 & 0 & 0 \\ -\omega_f^2\Delta t & 1 & 0 & 0 & 0 & 0 & 0 \\ 0 & 0 & 1 & \Delta t & 0 & 0 & 0 \\ 0 & 0 & -\omega_s^2\Delta t & 1 & 0 & 0 & 0 \\ 0 & 0 & 0 & 0 & 1 & 0 & 0 \\ 0 & 0 & 0 & 0 & 0 & 1 & 0 \\ 0 & 0 & 0 & 0 & 0 & 0 & 1 \end{pmatrix} \tag{8}$$

with $\omega_s = 2\pi \cdot f_s$ and $\omega_f = 2\pi \cdot f_f$ as the angular frequencies of the breathing frequency f_s and the heart beat rate f_f respectively.

Additionally, the measurement matrix $\mathbf{H}$, taken from (19), has to be updated. In the case of the present system, three different sensors are employed, see Fig. 1. Therefore, the measurement matrix $\mathbf{H}$ has to contain three different rows, see (9). Each sensor has its own state variable for the offset

$$\mathbf{H} = \begin{pmatrix} h_{f,1} & 0 & h_{s,1} & 0 & 1 & 0 & 0 \\ h_{f,2} & 0 & h_{s,2} & 0 & 0 & 1 & 0 \\ h_{f,3} & 0 & h_{s,3} & 0 & 0 & 0 & 1 \end{pmatrix} \tag{9}$$

The parameters $h_{f,1\cdots3}$ and $h_{s,1\cdots3}$ have been introduced to be able to weight the sensors differently during the fusion process. It highly depends on the signal quality of the sensor. So if e.g. all sensors are not corrupted, the absolute values of $h_{f,1\cdots3}$ and $h_{s,1\cdots3}$ will tend to 1. If one sensor is too noisy, its parameters will tend to 0. Negative values of parameters indicate that the sensor measures the "same" signal, but with inverted sign. To determine if a channel has good signal quality, the variance of the signals can be analysed,

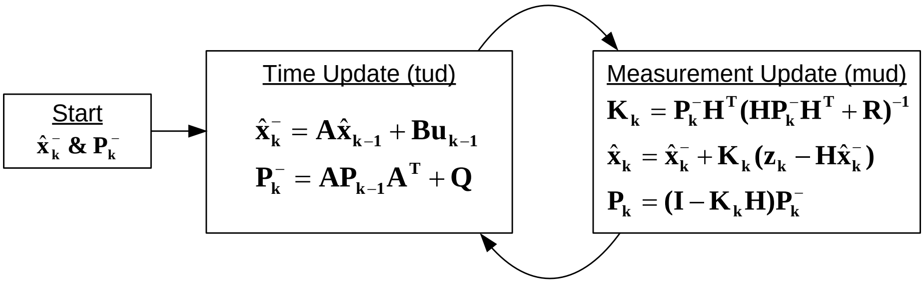

Fig. 2. Schematic way of iterative Kalman Filter parameter calculation ([2][8][9])

which would indicate high thoracic activity, always assuming that the signals are not corrupted by moving artefacts or measurement errors. For the sake of completeness it has to be said that the optional input signal $\mathbf{u_k}$ in (1) has not been used in the state model.

C. Signal Extraction

A major task in finding the optimal model parameters is the determination of the system and measurement noise $\mathbf{Q}$ and $\mathbf{R}$. In general, small values in the $\mathbf{Q}$ matrix mean a high smoothing and larger ones more adaptation to the (noisy) measured signal (with same $\mathbf{R}$ matrix). It also has been shown that higher sample rates achieve better filtering performance [11]. Good values for the matrix items in $\mathbf{R}$ can be set by evaluating the standard deviations ($\sigma_{1\cdots3}$) of each sensor without external stimulation (idle measurement):

$$\mathbf{R} = \begin{pmatrix} \sigma_1 & 0 & 0 \\ 0 & \sigma_2 & 0 \\ 0 & 0 & \sigma_3 \end{pmatrix} \tag{10}$$

III. Results and Discussion

The Kalman Filtering procedure has been applied to a real measurement set-up. It includes three different non-contacting sensors, placed on back of the body without any direct contact to the person. The sensors are based on measuring general impedance changes in the body due to thoracic activity, including breathing and heart beat. The detailed technical description of the sensory functioning is not part of this paper.

In addition to those signals, an airflow sensor attached to a breathing mask (FlowSensor) and a pulse-oximetry finger clip sensor (PPG) have been recorded as global references for respiration and heart beat activity (see Fig. 3). All the sensor signals have been recorded in parallel with a sample rate of 30 Hz. In time domain, the respiratory signal can be recognised in all raw sensor signals. The heart activity is not clearly visible, but present, as correlation analysis to the reference signal in the frequency domain have shown. It turned out that the amplitude change of the heart activity is about 1% compared to the breathing signal amplitude. This encourages to define the higher frequency components in the measurement matrix as $h_{f,1\cdots3} = 0.01 \cdot h_{s,1\cdots3}$ to reduce the amount of tunable parameters. For the measurement extract of 20 seconds in Fig. 3, best results were obtained with $h_{s,1\cdots3} = \begin{pmatrix} -0.44 & 0.29 & 0.27 \end{pmatrix}$. This measurement shows the case of one sensor (Sensor 1) measuring the breathing signal with inverted sign compared to Sensor 2 and 3. This effect can be seen best in the first three plots at $t = 38\ s$ on the time scale. Sensor 1 also has the best signal shape, thus giving it more influence in the measurement matrix.

Unfortunately, depending on the location of the sensor, unpredictable drifting, undesired body movements (artefacts) and different measurement principles - of course all of them having their benefits and drawbacks - unwanted noise is induced. These effects have to be considered in the processing algorithms. Due to the complexity of the specified facts, the standard deviation of the noise could not be determined accurately. Therefore, for simplicity reasons, the values for $\sigma_{1\cdots3}$ were set to 1, assuming equal sensor noise.

The last necessary system design has to be performed on the $\mathbf{Q}$ matrix. In fact, the three sensor offset states $C_{k,1\cdots3}$ represent the average of the recorded signal, which yields to low matrix values for the last three states, as stated in chapter II-C. For respiratory and beat activity, this smoothing has to be reduced by increasing the matrix values for the corresponding states. Good results could be achieved using the matrix in (11).

$$\mathbf{Q} = \begin{pmatrix} 1000 & 0 & 0 & 0 & 0 & 0 & 0 \\ 0 & 1000 & 0 & 0 & 0 & 0 & 0 \\ 0 & 0 & 100 & 0 & 0 & 0 & 0 \\ 0 & 0 & 0 & 100 & 0 & 0 & 0 \\ 0 & 0 & 0 & 0 & 10 & 0 & 0 \\ 0 & 0 & 0 & 0 & 0 & 10 & 0 \\ 0 & 0 & 0 & 0 & 0 & 0 & 10 \end{pmatrix} \tag{11}$$

Until this point, the values for the heart beat and breathing rate, f_f and f_s respectively, were not included into the model. The Kalman Filter is only as good as its model. Therefore, it is crucial to set f_f and f_s correctly to obtain best results. In general, these two values are not known, so that they have to be guessed. Fig. 3(a) and Fig. 3(b) show the cases that the breathing frequency has been set correctly ($f_s = 0.26\ Hz$) and consciously wrong ($f_s = 0.6\ Hz$), respectively. It is clearly visible that the filtering performance of the respiratory signal is highly degraded. As the frequency has been estimated much too high in the second case, higher frequency components can also be found at the Kalman Filter output compared to the first case. Nevertheless, the extraction of the heart beat signal is hardly affected. Also the extraction of this signal with very low amplitude, nearly invisible in the time domain of the raw data, has been achieved.

Another point of view of this signal processing algorithm is the real-time ability. In medical systems, especially whilst

ISBN: 978-988-19251-4-5
ISSN: 2078-0958 (Print); ISSN: 2078-0966 (Online)

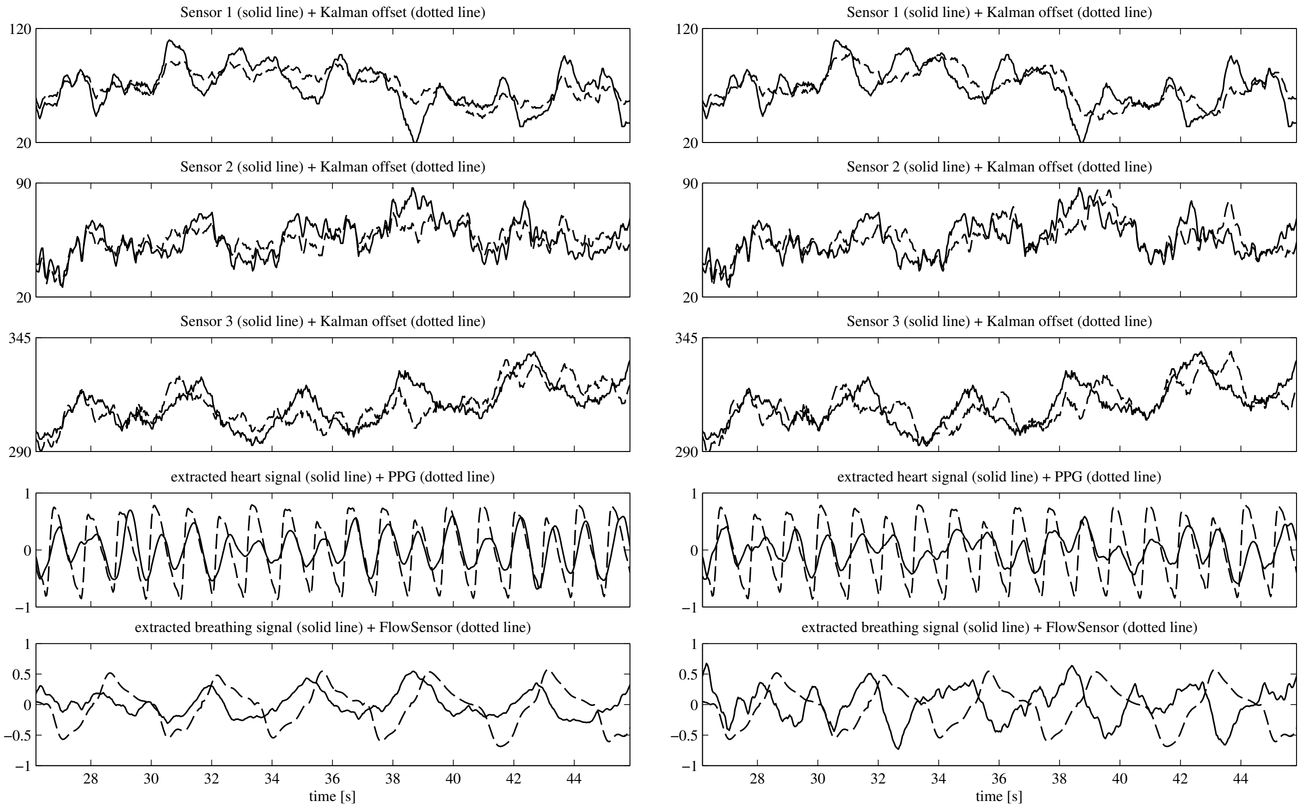

(a) Good breathing and heart frequency estimations (with $f_s = 0.26\ Hz$ and $f_f = 0.9\ Hz$).

(b) Poor breathing frequency and good heart frequency estimations (with $f_s = 0.6\ Hz$ and $f_f = 0.9\ Hz$.

Fig. 3. Kalman Filter results showing the three sensor signals and extracted vital signals with references (arbitrary units)

monitoring vital parameters, it is often desired to process signals as fast as possible. Therefore, the calculations, algorithms and visual display should not delay the original signal. In this work, the analysis has been performed offline. Nevertheless, it is possible to make a conclusion on this point by measuring the total processing time of a large data set. The calculation time of a 120 second data segment took about 2-3 seconds on a standard workstation (DualCore Intel®Pentium 4 at 2.4 GHz CPU frequency and 2 GB RAM). This already shows that even with seven states in the state vector, it is possible to do the signal processing in real-time. It also means, that an expansion to higher sampling rates is imaginable, resulting in even better filtering performance as the linearisation process is more accurate.

IV. Conclusion

Within this paper it has been shown that the Kalman Filtering technique allows to fuse sensors, extract signals and filter them directly in one processing block and in real-time. Nearly all matrices can be determined empirically. The only drawback is the missing knowledge about the correct frequencies f_f and f_s in the state transition matrix $\mathbf{A}$. A certain misalignment is tolerable, but the better the correlation frequencies to the real signal frequency the better the performance of the whole filtering. This issue can be solved by extending the linear state transition behaviour to a non-linear and adaptive transfer function (also called Extended Kalman Filter [8]). The missing frequencies would then also be estimated. Another approach is to use independent Kalman Filters for each sensor signal in a de-centralised configuration and to merge the outputs. In [9] it has been shown that the estimations of the states can then be improved.

Appendix
Derivation of state transition matrix and state vector

The following derivation has been taken and adapted from P. Spincemaille et al. [11]. They introduced a *periodic motion model*. The state transition matrix $\mathbf{A}$ and the state vector $\mathbf{x_k}$ can be derived as followed (assuming only one measurement signal as measurement). A signal $X(t)$ changing with the speed $V(t) = \frac{dX(t)}{dt}$ can be approximated by using the first Taylor polynomial. Assuming small time steps Δt, the inverse of the sampling frequency F_s, it results in:

$$X(t + \Delta t) \approx X(t) + \Delta t \frac{dX(t)}{dt} = \Delta t V(t) \qquad (12)$$

$$V(t + \Delta t) \approx V(t) + \Delta t \frac{dV(t)}{dt} \qquad (13)$$

Furthermore, we assume a *periodic sine shaped signal* with an angular frequency ω:

$$X(t) = sin(\omega \cdot t) \qquad (14)$$

Then, we obtain the speed $V(t)$ and its first derivative $\frac{dV(t)}{dt}$, which is again dependent on $X(t)$:

$$V(t) = \omega \cdot cos(\omega \cdot t) \qquad (15)$$

ISBN: 978-988-19251-4-5
ISSN: 2078-0958 (Print); ISSN: 2078-0966 (Online)

$$\frac{dV(t)}{dt} = -\omega^2 \cdot sin(\omega \cdot t) = -\omega^2 \cdot X(t) \qquad (16)$$

Inserted into (12) and (13), we obtain the discrete state vector and state transition matrix for one sine shaped signal. Often signals are biased with a constant or slowly changing offset that does not contain relevant information about the desired signal. To remove this offset, an additional state C_k is introduced, that contains the estimated offset value of the signal. Finally, the following state equations are defined:

$$\mathbf{x_k} = \begin{pmatrix} X_k \\ V_k \\ C_k \end{pmatrix} \qquad (17)$$

$$\mathbf{A} = \begin{pmatrix} 1 & \Delta t & 0 \\ -\omega^2 \Delta t & 1 & 0 \\ 0 & 0 & 1 \end{pmatrix}. \qquad (18)$$

The measured states in the filtering process in this case contain the desired signal in X_k and the undesired offset in C_k. Thus the measurement matrix $\mathbf{H}$ is set to:

$$\mathbf{H} = \begin{pmatrix} 1 & 0 & 1 \end{pmatrix}. \qquad (19)$$

The noise covariance matrices $\mathbf{Q}$ and $\mathbf{R}$ are strongly dependant on the applied measurement system. Therefore, no values are given at this point. For concrete values, see chapter III.

REFERENCES

[1] R. Kalman, “A new approach to linear filtering and prediction problems,” *Transactions of the ASME-Journal of Basic Engineering*, vol. 82, no. 1, pp. 35–45, 1960.

[2] B. Köhler, *Konzepte der statistischen Signalverarbeitung*. Berlin, Heidelberg: Springer-Verlag, 2005.

[3] Q. Li, R. G. Mark, and G. D. Clifford, “Robust heart rate estimation from multiple asynchronous noisy sources using signal quality indices and a Kalman filter,” *Physiol Meas.*, vol. 29, no. 1, pp. 15–32, Jul. 2008.

[4] M. Mneimneh, E. Yaz, M. Johnson, and R. Povinelli, “An adaptive Kalman filter for removing baseline wandering in ECG signals,” in *IEEE Computers in Cardiology, 2006*. Valencia, Spain: IEEE, 2006, pp. 253–256.

[5] O. Sayadi and M. B. Shamsollahi, “ECG denoising and compression using a modified extended Kalman filter structure.” *IEEE transactions on bio-medical engineering*, vol. 55, no. 9, pp. 2240–8, Sep. 2008.

[6] a. Schlogl, J. Fortin, W. Habenbacher, and M. Akay, “Adaptive mean and trend removal of heart rate variability using Kalman filtering,” *2001 Conference Proceedings of the 23rd Annual International Conference of the IEEE Engineering in Medicine and Biology Society*, pp. 571–573, 2001.

[7] B. Bracio, W. Horn, and D. Moller, “Sensor fusion in biomedical systems,” *Proceedings of the 19th Annual International Conference of the IEEE Engineering in Medicine and Biology Society. 'Magnificent Milestones and Emerging Opportunities in Medical Engineering' (Cat. No.97CH36136)*, vol. 1387, no. C, pp. 1387–1390, 1997.

[8] G. Welch and G. Bishop, “An introduction to the Kalman filter,” pp. 1–16, 1995.

[9] L. Drolet, F. Michaud, and J. Côté, “Adaptable sensor fusion using multiple Kalman filters,” in *Intelligent Robots and Systems, 2000.(IROS 2000). Proceedings. 2000 IEEE/RSJ International Conference on*, vol. 2. Takamatsu, Japan: IEEE, 2000, pp. 1434–1439.

[10] I. Hasu, “KALMAN FILTERING IN MULTI-SENSOR FUSION,” Ph.D. dissertation, Helsinki University of Technology, Finland, 2004.

[11] P. Spincemaille, T. D. Nguyen, M. R. Prince, and Y. Wang, “Kalman filtering for real-time navigator processing.” *Magnetic resonance in medicine : official journal of the Society of Magnetic Resonance in Medicine / Society of Magnetic Resonance in Medicine*, vol. 60, no. 1, pp. 158–68, Jul. 2008.

ISBN: 978-988-19251-4-5
ISSN: 2078-0958 (Print); ISSN: 2078-0966 (Online)